Nitrogen Reduction Hot Paper

How to cite: *Angew. Chem. Int. Ed.* **2022,** *61,* e202209899
International Edition: doi.org/10.1002/anie.202209899
German Edition: doi.org/10.1002/ange.202209899

Molecular Electrochemical Reductive Splitting of Dinitrogen with a Molybdenum Complex**

Lydia Merakeb, Soukaina Bennaamane, Jérémy De Freitas, Eric Clot, Nicolas Mézailles, and Marc Robert**

Abstract: Nitrogen reduction under mild conditions (room *T* and atmospheric *P*), using a non-fossil source of hydrogen remains a challenge. Molecular metal complexes, notably Mo based, have recently been shown to be active for such nitrogen fixation. We report electrochemical N_2 splitting with a Mo^{III} triphosphino complex [(PPP)MoI_3], at room temperature and a moderately negative potential. A Mo^{IV} nitride species was generated, which is confirmed by electrochemistry and NMR studies. The reaction goes through two successive one electron reductions of the starting Mo species, coordination of a N_2 molecule, and further splitting to a Mo^{IV} nitride complex. Preliminary DFT studies support the formation of a bridging $Mo^{I}N_2Mo^{I}$ dinitrogen dimer evolving to the Mo nitride via a low energy transition state. This example joins a short list of molecular complexes for N_2 electrochemical reductive cleavage. It opens a door to electrochemical proton-coupled electron transfer (PCET) conversion studies of N_2 to NH_3.

[*] Dr. L. Merakeb, J. De Freitas, Prof. M. Robert
Laboratoire d'Electrochimie Moléculaire—UMR 7591, Université Paris Cité
15, rue Jean Antoine de Baïf, 75013 Paris (France)
E-mail: robert@u-paris.fr

Dr. S. Bennaamane, Dr. N. Mézailles
Laboratoire Hétérochimie Fondamentale et Appliquée—UMR 5069, Université Toulouse III—Paul Sabatier
118, route de Narbonne, Bât 2R1, 31062 Toulouse (France)
E-mail: mezailles@chimie.ups-tlse.fr

Dr. E. Clot
ICGM, Univ Montpellier, CNRS, ENSCM
34000 Montpellier (France)

Prof. M. Robert
Institut Universitaire de France (IUF)
75005 Paris (France)

[**] A previous version of this manuscript has been deposited on a preprint server (https://doi.org/10.26434/chemrxiv-2021-dwvbg).

Nitrogen is one of the essential elements for life.[1] Although abundant, it is nonetheless a limiting nutrient in agriculture, and crop growth is dependent on its availability.[2] It is not only essential to the global economy as a fertilizer but also as the feedstock for industrial production of all N containing derivatives. Moreover, it has been identified as an alternative fuel as well as an energy storage molecule.[3,4] Today, ca. 200 million tons of NH_3 are produced yearly, exclusively by the Haber-Bosch (H–B) process [Eq. (1)].

$$N_2 + 3H_2 \rightleftharpoons 2NH_3 \qquad \Delta_r G^0 = -32.9\,kJ\,mol^{-1} \tag{1}$$

Although thermodynamically favorable, the reaction is carried out at high temperature (300–500 °C) and high pressure (200–300 bar) conditions over heterogeneous Fe containing catalysts, using ca. 1–2 % of the global energy production. It generates half a Gigaton of CO_2/year (ca. $^1/_2$ of the CO_2 generated is due to H_2 production by CH_4 reforming), a giant carbon footprint.

Nature, by means of microorganisms, transforms N_2 into NH_3 under ambient conditions, via multiple proton/electron transfers.[5] Nitrogenase enzymes, responsible for this "N_2 fixation" reaction [Eq. (2)], contain an organometallic active site, a $MoFe_7S_9C$-homocitrate cluster for the most common nitrogenase, which can be viewed as a homogeneous catalyst. The fact that this catalyst involves a coordination/activation of N_2 at one/several metal centers has spurred "organometallic chemists" to search for homogeneous catalysts able to achieve the N_2-to-NH_3 reaction efficiently.

$$N_2 + 8H^+ + 8e^- + 16ATP \rightleftharpoons 2NH_3 + H_2 + 16ADP + 16P_i \tag{2}$$

Transition metal complexes based on Mo[6–12] and Fe,[13–16] mainly, but also Re,[17–19] V,[20] Cr,[21–23] Co[24,25] and Ti[26] have been investigated in this purpose. However, a major hurdle toward such chemistry lies in the kinetically favorable proton reduction into H_2. Thus, despite several decades of active research, only a handful of catalysts are known for this reaction. Regarding electrochemical nitrogen splitting with molecular complexes,[27–29] an early example was identified by Picket and Talarmin with a W complex,[30] and in recent years, work has been performed on Ti[31] and Al[32] based complexes as well. The first example of electrochemically driven N_2-to-NH_3 catalytic conversion with a well-defined molecular species was reported in 2016. P_3^BFe-

(N_2)- (P_3^B = tris(o-diisopropylphosphinophenyl)borane) converts N_2 to NH_3 in Et_2O containing 0.1 M $Na[BAr^F_4]$ as a supporting electrolyte (BAr^F_4 = tetrakis(3,5-bis(trifluoromethyl)phenyl)borate) at −45 °C (Scheme 1a). With 50 equiv of $H[BAr^F_4]$ as a proton source and upon applying a potential of −2.3 V vs. Fc/Fc^+, 2.2 equiv of ammonia were produced with 25 % Faradaic efficiency over 16.5 h.[33]

Recently, partial electrochemical reduction of N_2 to hydrazine was shown at a tri-nickel based molecular catalyst. In THF (0.1 M Bu_4NPF_6), N_2 was converted into N_2H_4 at −2.35 V vs. Fc/Fc^+ with 8 to 12 % Faradaic efficiency, in the presence of 0.1 M phenol as a proton source (Scheme 1b).[34] Most recently, Peters demonstrated tandem electrochemical PCET (proton-coupled electron transfer) for N_2 reduction reaction (scheme 1c). Using a cobalt PCET mediator and Pickett's $[W(dppe)_2(N_2)_2]$ complex, N_2 was converted to up to 11.5 equiv of NH_3 at −1.35 V vs Fc/Fc^+ with 45 % FE (100 equiv TsOH as proton source, in DME).[35]

Electrochemical N_2 activation through splitting of the triple bond into metal nitrides has been recently the focus of several studies. Schneider, Siewert et al.[18] have used a Re^{III} complex for the electrochemical conversion into Re^V-nitride in 58 % yield at $E = -1.9$ V vs. Fc/Fc^+ in presence of dinitrogen (Scheme 1d). Using another rhenium complex with a similar but more conjugated pincer ligand led to N_2 splitting at a less cathodic potential, however at the expense of a lower yield which dropped to 15% (Scheme 1e).[36] Masuda et al. showed that splitting of dinitrogen into terminal nitrides is also possible by chemical and electrochemical oxidation of a N_2-bound Mo^0 complex (Scheme 1f).[37] Still regarding molybdenum, we have shown that the splitting of N_2 could be achieved through the two electron reduction of a $(PPP)MoCl_3$ complex (Scheme 2a) in the presence of NaI, and subsequently studied the functionalization of the nitride complex by silanes and boranes.[10]

These experimental studies, coupled to DFT calculations demonstrated the possible transformation of the nitride to imido (boryl and silyl) and to amido derivatives, which are related to the key intermediates toward complete reduction to ammonia.[38] In this work, we achieved the electrochemical splitting of dinitrogen with a Mo^{III} tris-phosphino complex $(PPP)MoI_3$ (**Mo2**, Scheme 2b) that leads to the formation of the corresponding Mo–nitride complex, at room temperature and moderate potential.

The cyclic voltammetry of **Mo2** was performed in THF and in chlorobenzene, showing similar behavior (Figures 1 and 2, respectively). Under Ar, it shows four distinct features. As seen for example in THF (Figure 1), a first reduction wave was observed at −1.15 V vs. SCE. Compar-

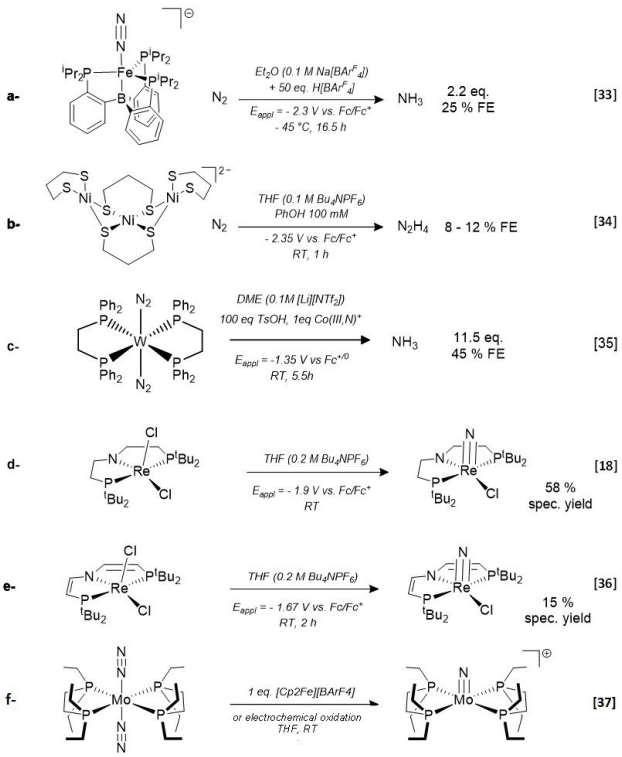

Scheme 1. Previous examples of molecular electrochemical reduction of N_2 to NH_3 (a), (c), hydrazine (b) or nitride complexes (d), (e).

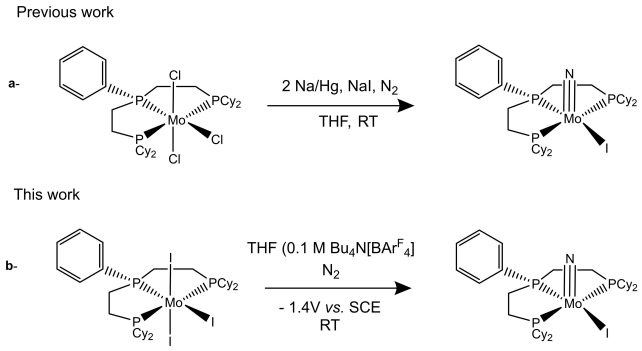

Scheme 2. Molybdenum complex for N_2 splitting in chemical (a) and electrochemical (b) conditions.

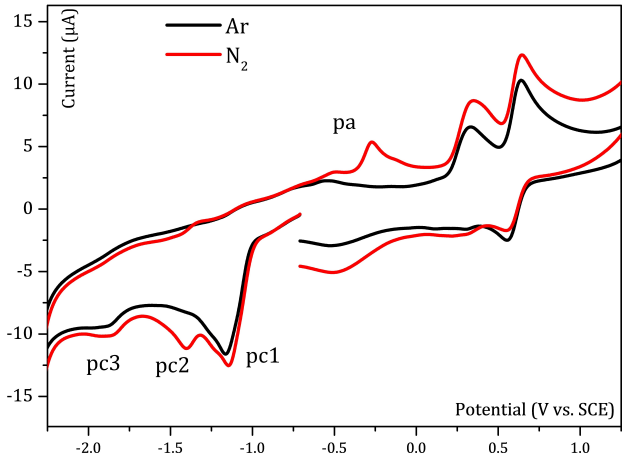

Figure 1. CVs of **Mo2** (0.58 mM) in THF + 0.1 M $Bu_4N[BAr^F_4]$ at a glassy carbon electrode, under Ar (black) and N_2 (red), at $\nu = 100$ mV s^{-1} and room temperature (RT). The initial potential was set at a value of −0.75 V vs SCE and the scan started toward reduction.

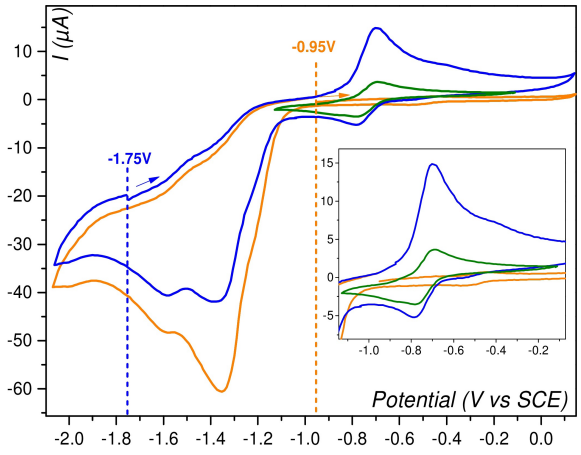

Figure 2. CVs of **Mo2** (4.4 mM) in THF + 0.1 M $Bu_4N[BAr^F{}_4]$ under N_2 atm, at $\nu = 100$ mV s^{-1} and RT. The starting potential, indicated with an arrow, was held for 15 s (orange and blue). Green trace: CV of **Mo3** (1.08 mM) in THF + 0.1 M $Bu_4N[BAr^F{}_4]$ under N_2 atm., at $\nu = 100$ mV s^{-1}, RT. Inset: zoomed view of the CV in the potential window where **Mo3** is oxidized.

ison to reversible couple of similar size shows that reduction is mono-electronic (ESI, Figure S6). It was further confirmed upon electrolysis experiment under Ar that the wave involves one electron exchange (ESI, Figure S9). It could thus be assigned to Mo^{III}/Mo^{II} couple.

Irreversibility of this wave (observed even at high scan rate) may be ascribed to a chemical step following the initial electron transfer, most likely iodide ligand dissociation. Indeed, oxidation waves at ca. 0.35 and 0.62 V (E^0, reversible) vs. SCE are observed, corresponding to I^- oxidation to I_2 and I_3^- respectively (see Figure S13). A second irreversible wave is located at −1.8 V vs. SCE (Figure 1, pc3). It may be noted that great care should be taken in the choice of supporting electrolyte anion. The classical hexafluorophosphate (PF_6^-) does coordinate to Mo, preventing any further reactivity with N_2 (ESI, Figure S5). The bulky, non-coordinating tetrakis(3,5-bis(trifluoromethyl)phenylborate ($BAr^F{}_4^-$) should be preferred.

Under an atmosphere of N_2, the cyclic voltammetry of **Mo2** shows additional features. A new reduction peak appears at −1.40 V vs. SCE in THF (Figure 1, pc2), along with a related oxidation peak at −0.26 V vs. SCE (Figure 1, pa). This later peak is only observed when the potential is scanned until pc2, thus it corresponds to the oxidation of a species formed at this later wave. Both waves are diffusion limited. The intensity of the first reduction peak (Figure 1, pc1) increases slightly and the peak potential is positively shifted under N_2, suggesting possible coordination to dinitrogen. The initial electrochemical behavior could be restored upon Ar bubbling.

The irreversible pc3 wave is not affected by the presence of N_2. We hypothesized that it could be due to the reduction of a small amount of Mo-oxo complex [(PPP)Mo=O$(I)_2$]. Indeed, an authentic sample of the synthesized oxo complex gave a CV reductive signal at similar potential than pc3 (Figure S14) and ^{31}P NMR confirmed the presence of a small quantity of the oxo species (two singlet peaks at 47 and 95 ppm), typically a few percent of the initial complex. Its presence may be due to traces of oxygen or water, or impurity. Likewise, NMR analysis after electrolysis (see below) does show an increase of the oxo complex signal (typically from ca. 3 % to 13 %, quantified by comparison with PPh_3 as an internal standard). The reduction of **Mo2** in chlorobenzene as solvent, also gives a reduction wave similar to pc3 due to the initial small amount of oxo species (Figure 2; note that redox waves are shifted to more negative potentials as compared to THF). In this solvent, electrolysis does not lead to an increase of the oxo concentration. Focusing on the species formed at pc2 and oxidized at pa, CVs of an authentic sample of **Mo3** were recorded in the same conditions. Oxidation of this complex occurs at the exact same potential as the species formed at pc2, as shown in Figure 2 and Figure S15, recorded in chlorobenzene and in THF respectively.

This indicates the likely formation of the nitride complex **Mo3** at pc2 reductive wave. To further investigate and demonstrate N_2 reductive splitting, a controlled potential electrolysis (CPE) of a THF solution (+0.1 M $Bu_4N[Bar^F{}_4]$) containing **Mo2** and saturated with N_2 was performed at −1.4 V vs. SCE, i.e. at pc2 peak potential. After a few minutes, coloration of the electrolyte solution changed from orange to greenish. After 35 min, a charge of 1.03 C was exchanged, corresponding to 1.24 e^- per Mo centre (see ESI for details). At the end of the electrolysis, cyclic voltammetry of the electrolyte solution was performed. The oxidation waves observed at ca. 0.5 and 0.75 V vs. SCE correspond to oxidation of iodide ions to I_2 and I_3^- along with a reduction wave at ca. −1.75 V vs. SCE, corresponding to the pc3 wave. Most importantly, a new reversible wave is observed at −0.31 V vs. SCE (Figure 3a). This wave corresponds to the reversible oxidation of Mo^{IV} nitride complex **Mo3**, electrochemically generated during the CPE. Indeed, comparison with CVs of an authentic sample of **Mo3** yields a reversible wave at the exact same potential (Figure 3a).

^{31}P NMR provided further characterization of the nitride complex.[39] After the CPE, the electrolyte solution was concentrated in a J-Young NMR tube, and a small volume of deuterated THF was added. Figure 3b shows two singlet peaks at 69 and 121 ppm respectively, which are characteristic of complex **Mo3** as deduced from comparison with the $^{31}P\{^1H\}$ spectrum of an authentic sample **Mo3**. The two additional singlet peaks observed at 53 and 98 ppm correspond to the signal of oxo species, as already discussed.

When the electrolysis experiment was performed under an Ar atmosphere, **Mo3** complex was not formed, as neither the reversible wave at −0.31 V vs. SCE in cyclic voltammetry, nor the signals at 69 and 121 ppm in $^{31}P\{^1H\}$ NMR were observed. Similar results were obtained in chlorobenzene under both Ar and N_2.

Combined CV and ^{31}P NMR data converge to the robust conclusion that **Mo3** is obtained from **Mo2** and dinitrogen upon electrochemical reduction. The chemical yield of the reaction could be derived from cyclic voltammetry by comparing the intensity of the observed reversible wave at −0.31 V after CPE with a CV recorded in the same

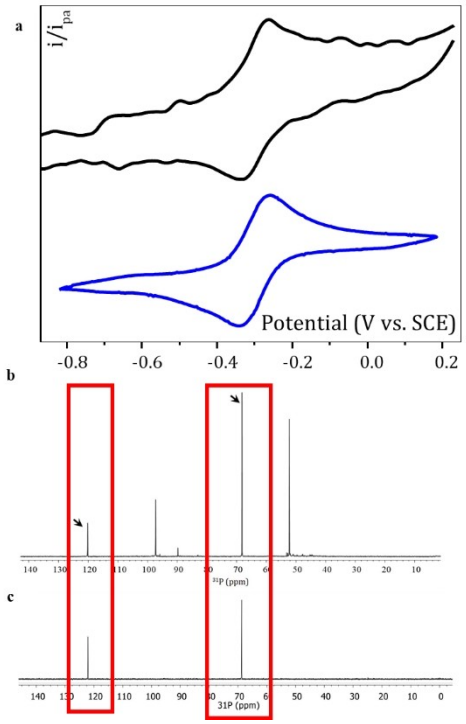

Figure 3. a) CV at 1 mm GC disk of the electrolyte solution after CPE (black) of **Mo2** (2.46 mM) and CV at 3 mm GC disk of **Mo3** (1.12 mM) in THF + 0.1 M $Bu_4N[BAr^F{}_4]$ under N_2 atm., at $\nu = 100$ mV s^{-1}, RT. b) $^{31}P\{^1H\}$ NMR of the same electrolyte solution. c) $^{31}P\{^1H\}$ NMR of complex **Mo3** in THF d-8.

electrolyte conditions, before CPE. The chemical yield was thus found to be ca. 30 % based on the Mo. Since the charge passed during the electrolysis was 1.24 e$^-$ per Mo, less than the 2 e$^-$/Mo required for the full conversion of **Mo2** to **Mo3**, the Faradaic yield for **Mo3** production is equal to 49 %. The fact that **Mo2** is not fully converted into **Mo3** could be expected from inspection of data in Figures 1 and 2. Indeed, the intensity of the pc2 wave, at which **Mo3** is produced, is significantly smaller than that of the one electron pc1 wave.

Preliminary DFT calculations were carried out to get insights into the reaction mechanism (Scheme 3, gas phase optimization PBE0-D3/Def2SVP and solvent energy calculations (SMD, THF) at PBE0/Def2QZVP, see ESI for details). Relative energies between Mo complexes with different redox states were estimated using Cp^*_2Co as a one electron reducing agent. This choice has been motivated because the redox potential of $Cp^*_2Co^+/Cp^*_2Co$ (−1.84 V in THF, computed at −2.1 V) and the position of the reduction wave pc1 (−1.95 V vs. Fc^+/Fc) are close. The lowest potential energy surface (PES) (lowest energy complexes with corresponding spin state) is presented. Complexes in different spin states have been computed and are mentioned when relevant. Calculations start with the **Mo2** complex ^{4}**A**, a quartet of spin. One electron reduction leads to the anionic complex ^{5}**B** (quintet of spin) in a mildly exergonic process (−3.4 kcal mol^{-1}). Interestingly, one of the Mo–I apical bonds is strongly elongated in ^{5}**B** (5.38 Å), and thus the unsaturated complex ^{5}**C** [(PPP)MoI_2] lies close in energy (−0.6 kcal mol^{-1} with respect to ^{5}**B**). Calculations could not locate a local extremum associated to N_2 coordinated to ^{5}**C**. As observed in the tri-iodide structure, octahedral geometry is not favored with a quintet spin state (Mo···N_2 distance of 4.45 Å). However, the complex ^{3}**C** with a triplet spin state lies slightly above ^{5}**C** (−2.8 and −4.0 kcal mol^{-1} respectively) and coordination of N_2 to this complex is a kinetically facile step. Indeed, the transition state **TS(^{3}C-^{3}D)** is located only 15.9 kcal mol^{-1} higher than ^{3}**C**. Dinitrogen Mo^{II} complex ^{3}**D** is only 1.6 kcal mol^{-1} higher than ^{3}**C**, and these two complexes are therefore in equilibrium. Splitting of N_2 was evaluated at the Mo^{II} redox state. Reaction between ^{3}**C** and ^{3}**D** to form a dimer ^{3}**C-D** (triplet spin state) or ^{1}**C-D** (singlet spin state) is computed to be endergonic with respect to ^{3}**C** and ^{3}**D** ($\Delta G = 9.6$ kcal mol^{-1}, ^{1}**C-D**; $\Delta G = 4.9$ kcal mol^{-1}, ^{3}**C-D**). Moreover, calculations of the transition states for N_2 cleavage for both dimers resulted in very high activation energies ($\Delta G^{\neq} = 52.0$ kcal mol^{-1}, from ^{1}**C-D**; $\Delta G^{\neq} = 37.3$ kcal mol^{-1}, from ^{3}**C-D**), and such pathway can be discarded.

One electron reduction of ^{3}**C** and ^{3}**D** is computed to be endoergic by $\Delta G = 5.4$ kcal mol^{-1} and $\Delta G = 6.1$ kcal mol^{-1}, respectively. The reduced species are more stable as doublet spin states and iodide dissociation yields the mono-iodo complex [(PPP)MoI] (^{2}**E**) and ^{2}**F** from coordination to N_2. The combined reduction/iodide dissociation is computed to be endoergic in the case of ^{3}**C**→^{2}**E**+**I**$^-$ ($\Delta G = 4.3$ kcal mol^{-1}), whereas it is slightly exoergic in the case of ^{3}**D**→^{2}**F**+**I**$^-$ ($\Delta G = -0.4$ kcal mol^{-1}). Contrary to the situation encountered with Mo^{II} center, the Mo^I-N_2 complex ^{2}**F** is computed to be more stable than the unsaturated Mo^I complex ^{2}**E** by $\Delta G = -3.1$ kcal mol^{-1}. As a result of this additional stability, the N_2 coordination to ^{2}**E** is computed to be favorable ($\Delta G^{\neq} = 8.4$ kcal mol^{-1}) to yield ^{2}**F**. Formation of dimer species between ^{2}**E** and ^{2}**F**, either as a singlet (^{1}**E-F**) or as a triplet (^{3}**E-F**) is computed to be exergonic ($\Delta G = -15.2$ kcal mol^{-1}, ^{1}**E-F**; $\Delta G = -15.4$ kcal mol^{-1}, ^{3}**E-F**). Despite being close in energy, the N_2 cleavage is operative only from the singlet dimer ^{1}**E-F** with an activation barrier of $\Delta G^{\neq} = 21.0$ kcal mol^{-1}, whereas the process is computed to be highly unfavorable from the triplet dimer ($\Delta G^{\neq} = 65.0$ kcal mol^{-1}). The singlet transition state exhibits an expected zig-zag geometry with a highly elongated N–N bond (1.631 Å vs. 1.192 Å in ^{1}**E-F**) and shorter Mo–N contacts (1.689 Å and 1.693 Å vs. 1.868 Å and 1.871 Å in ^{1}**E-F**). The overall transformation ^{2}**E** + ^{2}**F** → 2 ^{1}**G**, where ^{1}**G** is the Mo^{IV}-nitrido (**Mo3**) final product resulting from N_2 cleavage is computed to be strongly exoergic ($\Delta G = -55.3$ kcal mol^{-1}).

Overall, DFT studies support the electrochemical mechanism for N_2 splitting given in Scheme 4. It involves spontaneous iodide dissociation upon one-electron reduction to form the Mo^{II} di-iodide intermediate in equilibrium with the N_2-coordinated Mo^{II} complex. Mo^{II} N_2-dimer formation is thermodynamically accessible but N_2 cleavage is kinetically prohibited. A second reduction at more negative potential results in further iodide dissociation and easy N_2 coordination to Mo^I, resulting in thermodynamically easy formation of N_2-dimer species from which splitting to Mo^{IV} nitride species is kinetically accessible.

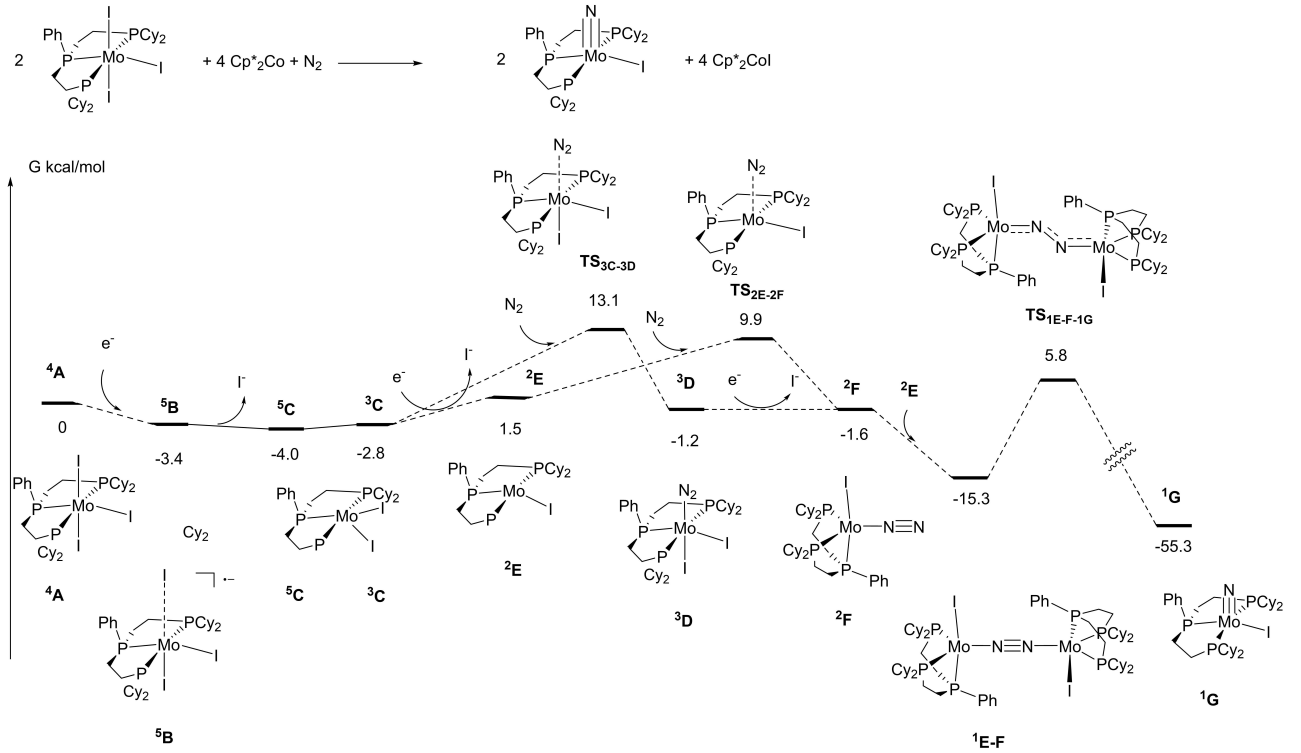

Scheme 3. DFT mechanism insights into reductive N_2 splitting with **Mo2**.

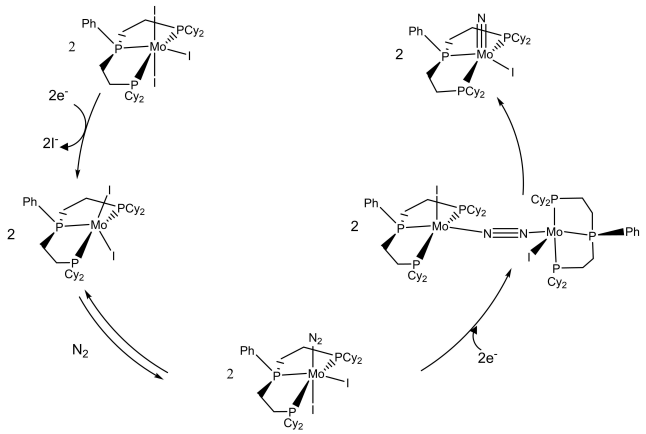

Scheme 4. Plausible mechanism for electrochemical reduction of N_2 with **Mo2** complex.

In summary, we have demonstrated the electrochemical splitting of dinitrogen at a Mo molecular complex under ambient conditions, and characterized the formation of the corresponding Mo nitride complex, which was obtained in 30 % chemical yield (49 % Faradaic efficiency). Such nitride complexes are an ideal starting point not only for chemical functionalization but also and most importantly for electrochemical studies aiming at generating ammonia by successive proton-coupled electron transfers (PCET process), one step closer from molecular electrochemical catalysis of N_2 reduction with metal complexes. Such studies will be reported in due time.

Acknowledgements

Authors would like to acknowledge support from the Agence Nationale de la Recherche (ANR) through the program ANR-16-CE07-0033-04. Partial financial support to M.R. from the Institut Universitaire de France (IUF) is gratefully acknowledged.

Conflict of Interest

The authors declare no conflict of interest.

Data Availability Statement

The data that support the findings of this study are available from the corresponding author upon reasonable request.

Keywords: Dinitrogen Reductive Splitting · Electrochemical Reduction of N_2 · Molybdenum Complex · Nitride Mo Complex

[1] S. J. Ferguson, *Curr. Opin. Chem. Biol.* **1998**, *2*, 182–193.
[2] N. Gruber, J. N. Galloway, *Nature* **2008**, *451*, 293–296.
[3] J. Guo, P. Chen, *Chem* **2017**, *3*, 709–712.
[4] R. Lan, J. T. S. Irvine, S. Tao, *Int. J. Hydrogen Energy* **2012**, *37*, 1482–1494.
[5] B. M. Hoffman, D. Lukoyanov, Z. Y. Yang, D. R. Dean, L. C. Seefeldt, *Chem. Rev.* **2014**, *114*, 4041–4062.

[6] D. V. Yandulov, R. R. Schrock, *Science* **2003**, *301*, 76–78.
[7] L. A. Wickramasinghe, T. Ogawa, R. R. Schrock, P. Müller, *J. Am. Chem. Soc.* **2017**, *139*, 9132–9135.
[8] K. Arashiba, Y. Miyake, Y. Nishibayashi, *Nat. Chem.* **2011**, *3*, 120–125.
[9] Y. Ashida, K. Arashiba, K. Nakajima, Y. Nishibayashi, *Nature* **2019**, *568*, 536–540.
[10] Q. Liao, A. Cavaillé, N. Saffon-Merceron, N. Mézailles, *Angew. Chem. Int. Ed.* **2016**, *55*, 11212–11216; *Angew. Chem.* **2016**, *128*, 11378–11382.
[11] G. A. Silantyev, M. Förster, B. Schluschaß, J. Abbenseth, C. Würtele, C. Volkmann, M. C. Holthausen, S. Schneider, *Angew. Chem. Int. Ed.* **2017**, *56*, 5872–5876; *Angew. Chem.* **2017**, *129*, 5966–5970.
[12] A. S. Bennaamane, M. F. Espada, A. Mulas, T. Personeni, N. Saffon-merceron, M. Fustier-Boutignon, C. Bucher, N. Mézailles, *Angew. Chem. Int. Ed.* **2021**, *60*, 20210; *Angew. Chem.* **2021**, *133*, 20372.
[13] J. S. Anderson, J. Rittle, J. C. Peters, *Nature* **2013**, *501*, 84–87.
[14] M. Reiners, D. Baabe, K. Münster, M. K. Zaretzke, M. Freytag, P. G. Jones, Y. Coppel, S. Bontemps, I. del Rosal, L. Maron, M. D. Walter, *Nat. Chem.* **2020**, *12*, 740–746.
[15] R. B. Ferreira, B. J. Cook, B. J. Knight, V. J. Catalano, R. García-Serres, L. J. Murray, *ACS Catal.* **2018**, *8*, 7208–7212.
[16] S. F. McWilliams, P. L. Holland, *Acc. Chem. Res.* **2015**, *48*, 2059–2065.
[17] I. Klopsch, M. Finger, C. Würtele, B. Milde, D. B. Werz, S. Schneider, *J. Am. Chem. Soc.* **2014**, *136*, 6881–6883.
[18] B. M. Lindley, R. S. Van Alten, M. Finger, F. Schendzielorz, C. Würtele, A. J. M. Miller, I. Siewert, S. Schneider, *J. Am. Chem. Soc.* **2018**, *140*, 7922–7935.
[19] Q. J. Bruch, G. P. Connor, C. H. Chen, P. L. Holland, J. M. Mayer, F. Hasanayn, A. J. M. Miller, *J. Am. Chem. Soc.* **2019**, *141*, 20198–20208.
[20] Y. Sekiguchi, K. Arashiba, H. Tanaka, A. Eizawa, K. Nakajima, K. Yoshizawa, Y. Nishibayashi, *Angew. Chem. Int. Ed.* **2018**, *57*, 9064–9068; *Angew. Chem.* **2018**, *130*, 9202–9206.
[21] A. J. Kendall, S. I. Johnson, R. M. Bullock, M. T. Mock, *J. Am. Chem. Soc.* **2018**, *140*, 2528–2536.
[22] T. Shima, J. Yang, G. Luo, Y. Luo, Z. Hou, *J. Am. Chem. Soc.* **2020**, *142*, 9007–9016.
[23] A. J. Kendall, M. T. Mock, *Eur. J. Inorg. Chem.* **2020**, 1358–1375.
[24] S. Kuriyama, K. Arashiba, H. Tanaka, Y. Matsuo, K. Nakajima, K. Yoshizawa, Y. Nishibayashi, *Angew. Chem. Int. Ed.* **2016**, *55*, 14291–14295; *Angew. Chem.* **2016**, *128*, 14503–14507.
[25] T. Suzuki, K. Fujimoto, Y. Takemoto, Y. Wasada-Tsutsui, T. Ozawa, T. Inomata, M. D. Fryzuk, H. Masuda, *ACS Catal.* **2018**, *8*, 3011–3015.
[26] L. R. Doyle, A. J. Wooles, L. C. Jenkins, F. Tuna, E. J. L. McInnes, S. T. Liddle, *Angew. Chem. Int. Ed.* **2018**, *57*, 6314–6318; *Angew. Chem.* **2018**, *130*, 6422–6426.
[27] N. Ostermann, I. Siewert, *Curr. Opin. Electrochem.* **2019**, *15*, 97–101.
[28] Q. J. Bruch, G. P. Connor, N. D. McMillion, A. S. Goldman, F. Hasanayn, P. L. Holland, A. J. M. Miller, *ACS Catal.* **2020**, *10*, 10826–10846.
[29] M. J. Chalkley, M. W. Drover, J. C. Peters, *Chem. Rev.* **2020**, *120*, 5582–5636.
[30] C. J. Pickett, J. Talarmin, *Nature* **1985**, *317*, 652–653.
[31] E. Y. Jeong, C. Y. Yoo, C. H. Jung, J. H. Park, Y. C. Park, J. N. Kim, S. G. Oh, Y. Woo, H. C. Yoon, *ACS Sustainable Chem. Eng.* **2017**, *5*, 9662–9666.
[32] T. J. Sherbow, E. J. Thompson, A. Arnold, R. I. Sayler, R. D. Britt, L. A. Berben, *Chem. Eur. J.* **2019**, *25*, 454–458.
[33] T. J. Del Castillo, N. B. Thompson, J. C. Peters, *J. Am. Chem. Soc.* **2016**, *138*, 5341–5350.
[34] P. Saha, S. Amanullah, A. Dey, *J. Am. Chem. Soc.* **2020**, *142*, 17312–17317.
[35] P. Garrido-Barros, J. Derosa, M. Chalkley, J. Peters, Tandem electrocatalytic N_2 fixation via concerted proton-electron transfer. ChemRxiv. Cambridge: Cambridge Open Engage; 2021; This content is a preprint and has not been peer-reviewed.
[36] R. S. van Alten, F. Wätjen, S. Demeshko, A. J. M. Miller, C. Würtele, I. Siewert, S. Schneider, *Eur. J. Inorg. Chem.* **2020**, 1402–1410.
[37] A. Katayama, T. Ohta, Y. Wasada-Tsutsui, T. Inomata, T. Ozawa, T. Ogura, H. Masuda, *Angew. Chem. Int. Ed.* **2019**, *58*, 11279–11284; *Angew. Chem.* **2019**, *131*, 11401–11406.
[38] S. Bennaamane, M. F. Espada, I. Yagoub, N. Saffon-Merceron, N. Nebra, M. Fustier-Boutignon, E. Clot, N. Mézailles, *Eur. J. Inorg. Chem.* **2020**, 1499–1505.
[39] D. W. Meek, T. J. Mazanec, *Acc. Chem. Res.* **1981**, *14*, 266–274.

Manuscript received: July 7, 2022
Accepted manuscript online: August 8, 2022
Version of record online: August 25, 2022